Food & Function

ROYAL SOCIETY OF CHEMISTRY

PAPER

View Article Online
View Journal

Cite this: DOI: 10.1039/d4fo02442g

Effects of konjac glucomannan intake patterns on glucose and lipid metabolism of obese mice induced by a high fat diet†

Sijia Zhu, [a,b] Jiyu Yang,[a,b] Pengkui Xia,[a,b] Sha Li,[a,b] Qi Wang,[a,b] Kaikai Li, [a,b] Bin Li [a,b] and Jing Li *[a,b]

Konjac glucomannan (KGM) is a dietary fiber supplement that exhibits multiple biological activities, including weight control as well as regulation of glucose and lipid metabolism. Currently, KGM intake patterns in practical applications include KGM sol, thermal irreversible gel, and frozen thermal irreversible gel. In this study, four intake patterns of KGM, namely KGM sol (KS), deacetylated KGM (DK), KGM gel (KG), and frozen KGM gel (FKG), were used as materials to explore the effects of different KGM intake patterns on glucose and lipid metabolism and intestinal flora in obese mice induced by a high fat diet under the same dose. The results showed that any type of KGM intake could reduce body weight, fat mass, lipid levels, and insulin resistance in obese mice, and alleviate liver damage and inflammation caused by obesity. However, KS has the most significant effect on controlling blood glucose and blood lipid in obese mice. Additionally, it was found that KS, DK, KG and FKG can increase the α-diversity of intestinal microflora in high-fat mice and improve the microflora disorder in high-fat mice. Finally, KS may increase the levels of fasting appetite hormones GLP-1 and PYY in mice, up-regulate the expression of *LDLR*, *GCK* and *G-6-pase* mRNA, and increase the production of short-chain fatty acids (SCFAs) in the intestinal flora of mice, thus regulating glucose and lipid metabolism. This study systematically investigated the effects of different intake forms of KGM on metabolism and intestinal flora in obese mice, which is of great significance for further understanding the role of KGM in the prevention and treatment of obesity-related metabolic diseases and for developing targeted dietary interventions.

Received 24th May 2024,
Accepted 18th August 2024

DOI: 10.1039/d4fo02442g

rsc.li/food-function

1. Introduction

The global population of overweight and obese individuals is increasing rapidly, with around one in three people globally being diagnosed as overweight or obese.[1] Obesity and being overweight can lead to a dynamic increase in the incidence of diseases such as hypertension, type 2 diabetes, and ischaemia heart disease, with a 10–13% premature mortality rate directly attributable to obesity in Europe.[2] Obesity and being overweight not only bring serious physical and psychological trauma to individuals but also produce a huge social and economic burden, and have become unavoidable public health problems in industrialized countries.[3]

The development of obesity enlarges the body's fat cells and releases excess free fatty acids in the body.[4] When these excess systemic free fatty acids enter the cells of non-fat organs such as the liver, muscles and pancreas, they can cause ectopic fat deposition in the body and then produce lipid toxicity, further releasing excess reactive oxygen species and inflammatory factors and eventually leading to systemic inflammation.[5] Chronically low systemic inflammation blocks the action of insulin signaling pathways, thereby disrupting glucose homeostasis and leading to systemic dysregulation of glucose and lipid metabolism. In a final analysis, obesity is mainly caused by a long-term serious imbalance between the body's energy absorption and energy consumption. Therefore, it is crucial to limit energy intake and absorption for the treatment of obesity and being overweight. Increasing the intake of dietary fiber can reduce the utilization of nutrients, decrease energy absorption, and ultimately control body weight.

In recent years, the gut microbiome-targeting diet has attracted a lot of attention from researchers as a new way to increase microbiome diversity to combat and prevent obesity.[6] The gut microbiome encompasses a diverse array of symbiotic

[a]College of Food Science and Technology, Huazhong Agricultural University, Wuhan 430070, China. E-mail: lijingfood@mail.hzau.edu.cn
[b]Key Laboratory of Environment Correlative Dietology, Huazhong Agricultural University, Ministry of Education, China

† Electronic supplementary information (ESI) available. See DOI: https://doi.org/10.1039/d4fo02442g

microorganisms consisting of trillions of bacteria, fungi, and viruses. These microbes interact harmoniously with the host, and their metabolites significantly influence overall health. The gut microbiota plays a crucial role in overseeing metabolic, endocrine, and immune functions.[7] Diet is considered to be a key environmental factor mediating gastrointestinal microbiota composition and metabolic function.[8] Dietary fiber is not digested by host enzymes in the upper intestine but is metabolized by microorganisms in the cecum and colon. Short-chain fatty acids are the main products of this dietary fiber fermentation in the gut. Short-chain fatty acids act as mediators of various pathways, including local, immune and endocrine effects, and microbiota–gut–brain communication.[9] It is generally believed that dietary fiber improves glucose and lipid metabolism and prevents related diseases by involving the gut microbiota and increasing short-chain fatty acid metabolism pathways.

KGM is a water-soluble dietary fiber (DF) extracted from the tubers of the konjac plant. It consists of D-mannose and D-glucose in a ratio of 1.6 : 1 or 1.4 : 1, connected by β-1,4-glucosidic linkages, with a molecular weight ranging from 200 to 2000 kDa.[10,11] KGM is a kind of natural polysaccharide with unique structure and physicochemical properties, exhibiting significant biological value and potential applications. Pharmacological studies have shown that KGM possesses various activities, including anti-diabetic, anti-obesity, laxative, and prebiotic effects.[12] Numerous human studies have demonstrated that KGM can reduce postprandial glycemic fluctuations, improve lipid profiles, and contribute to combating obesity.[13–15] Animal studies have also indicated that KGM inhibits cholesterol synthesis in the liver and promotes the fecal excretion of cholesterol and bile acids.[16]

As a dietary fiber supplement, low oral doses of KGM can produce a great sense of satiety compared with other dietary fibers, and its addition to the body is well tolerated, with only mild gastrointestinal symptoms.[17] The versatile nature of KGM as a staple food in Asia is evident through its utilization in various forms such as noodles, tofu, and vegetarian meat, thereby presenting immense opportunities within the consumer market and application domains. It was concluded that sol, thermal irreversible gel, and frozen thermal irreversible gel were the main forms of ingestion. However, at the same dose, which KGM intake pattern is more effective for body health is unknown. Based on this, this study prepared common KGM products on the market; investigated their effects on appetite, glucose and lipid metabolism and intestinal microbiota; and evaluated their long-term anti-obesity effects to compare the bioavailability of KGM with different intake patterns.

2. Materials and methods

2.1. Preparation of various intake patterns of KGM

KGM (purity: 90%, M_w: 6.215 × 10^5 Da) was purchased from Hubei Konson Konjac Gum Co., Ltd (Wuhan, China). Other chemicals were purchased from Sinopharm Group Chemical Reagent Co., unless otherwise stated. The water used in this study was distilled water. The ELISA kit used in this study was purchased from Jiangsu Meimian Industrial Co., Ltd, and the biological kit was purchased from Nanjing Jiancheng Bioengineering Research Institute.

KGM sol (KS). A 4 g sample of konjac powder was added into 96 g of water, stirred well, and left to stand until it fully expanded to form konjac sol.

Deacetylated KGM (DK). DK was prepared according to Du *et al.*'s method.[18] A 30 g sample of KGM and 3.6 g of Na_2CO_3 were mixed with 150 ml of 50% ethanol in a conical bottle and reacted at constant temperature and with a shock at 40 °C for 24 h. At the end of the reaction, the crude product was immersed in twice the volume of 50% ethanol and then vacuum filtered. The sample was soaked and filtered several times until the pH was neutral. The samples were then dehydrated with 75% and 95% ethanol, respectively. Finally, the DK powder was obtained by vacuum drying at 40 °C for 6 h. Then, 4 g of DK powder was dispersed in 96 g of distilled water to make it fully swollen to form DK.

KGM gel (KG). A 2.4 g sample of Na_2CO_3 was added into 477.6 g of water. After Na_2CO_3 was completely dissolved, 20 g of KGM was added to the solution, which was then left to rest after stirring for about 2 min. The next day, the overnight sample was heated in a constant temperature water bath at 90 °C for 2 h. After heating, the sample was cooled at room temperature, and a KG gel block was formed when cooled to room temperature. In order to facilitate gavage and simulate the state after chewing, the prepared gel blocks were divided into small blocks of about 0.5 cm × 0.5 cm × 0.5 cm. To remove Na_2CO_3 in the gel, the gel was soaked in 0.2% citric acid solution for 10 min and fully rinsed with distilled water. The gel was repeatedly soaked in citric acid solution and rinsed with distilled water until the pH was neutral. The rinsed gel blocks were then crushed in a homogenizer for 5 min and then ground with a colloid mill for 20 min to obtain the finished konjac glucomannan gel.

Frozen konjac glucomannan gel (FKG). After the KG gel block was prepared, the KG gel was frozen at −20 °C for 12 h and thawed overnight at room temperature to obtain the FKG gel block. The following steps are the same as those for the preparation of KG, which are dividing into small pieces, acid soaking, washing, crushing and grinding.

2.2. Infrared spectroscopic analysis

The fully dried samples were mixed with potassium bromide at a mass ratio of about 1 : 100, ground in an agate mortar, and pressed into tablets. Before testing, potassium bromide without the samples was scanned and used to determine the background, which was subtracted from the sample during testing. An ATR accessory was used with a wave number range of 4000 to 400 cm^{-1}, a resolution of 4 cm^{-1}, and 32 scans.

2.3. Rheological properties analysis

A parallel aluminum plate with a diameter of 6 cm was selected, and the flow sweep program was used to detect the

flow behavior of the sol. The gap space was set to 500 μm, the shear rate scan range was 0.1–100 s^{-1}, and the temperature was 37 °C. In addition, the peak hold procedure was used to measure the apparent viscosity of the sol at a shear rate of 50 s^{-1}. To prevent evaporation of water, an insulation cover was used and methicone oil was applied to the cracks. TRIOS software (version 4.4041128) was used to obtain the data, and the built-in Williamson model of the software was used to fit and quantify the flow behavior of the sol.

2.4. Animal experiment design

All experimental procedures were carried out in accordance with the Chinese regulations on the management of laboratory animal affairs and confirmed by the Hubei Provincial Laboratory Animal Research Center and the Ethics Committee of Huazhong Agricultural University. Approval number: HZAUMO-2023-0171.

Seven-week-old male C57BL/6J mice (n = 60, weight = 18–20 g) were purchased from the Laboratory Animal Center of Huazhong Agricultural University and kept in the specific pathogen free (SPF)-rated animal house of the Laboratory Animal Center of Huazhong Agricultural University. The feeding environment temperature was 24–26 °C, the relative humidity was 60%, and the light and dark cycle was 12/12 h (light time 8:00–20:00). After changing the feeding environment, the mice were fed adaptively for one week. During the adaptation period, all the mice ate and drank freely. The food intake, drinking amount, and activity behavior of the mice were observed to detect whether abnormalities occurred.

After one week of adaptive feeding, all mice were randomly divided into six groups (10 mice per group, 5 mice per cage) based on their body weight, which were named as blank control group (recorded as C), high-fat diet control group (recorded as HF), konjac glucomannan sol group (recorded as KS), deacetylated konjac glucomannan group (recorded as DK), konjac glucomannan gel group (recorded as KG), and frozen konjac glucomannan gel group (recorded as FKG) (Fig. 1). The intragastric volume of the mice in this experiment was 1 mL per 100 g; the intragastric dose of the KS, DK, KG and FKG groups was 400 mg dry matter per kg body weight; and the mice in group C and HF were intragastrically administered with the same volume of distilled water.

After the end of the adaptation period, the mice in different groups were fed D12450J (low fat diet, group C diet) and D12492 (high fat diet, HF, KS, DK, KG and FKG diets) for intervention treatment. Both diets were purchased from ReadyDietech Company in China, and the diet formula is shown in Table S1.†

2.5. Sample collection

The bedding and feed were changed every two days, and the daily food intake and weekly body weight of the mice were recorded. During the last week of the experiment, fresh feces from each mouse were collected into sterile tubes. After 12 weeks of intervention feeding, all mice were anesthetized after 12 h of fasting. Blood samples were collected from the eyes of each mouse and allowed to stand at room temperature until the whole blood coagulated, followed by centrifugation at 3000 rpm for 10 min at 4 °C to rapidly separate serum. The mice were sacrificed by cervical dislocation, and the liver and adipose tissue were dissected. The liver and adipose tissues were washed in frozen saline, dried with filter paper, and weighed. Part of the liver and adipose tissue was locally fixed with 4% paraformaldehyde solution for histological observation. Serum samples and the remaining liver and adipose tissue were packaged, rapidly frozen in liquid nitrogen, and transferred to a freezer at −80 °C for storage.

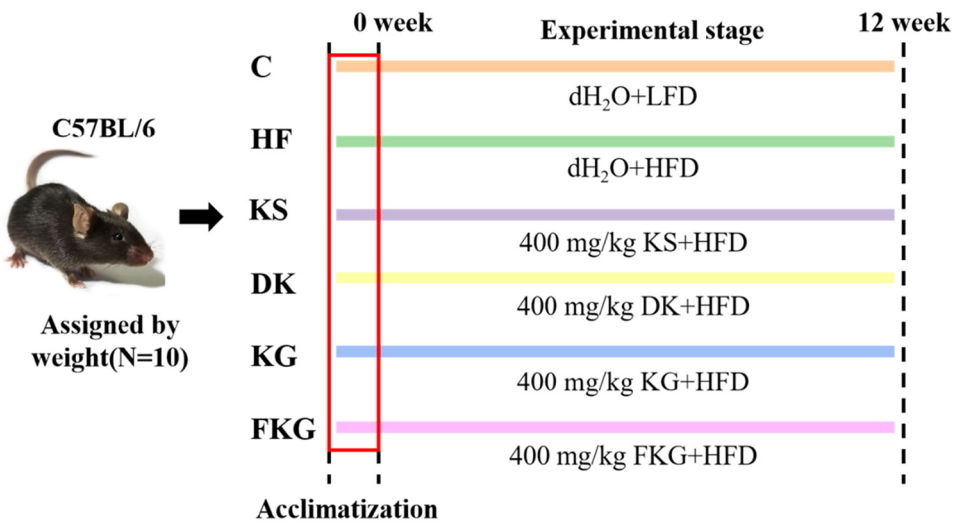

Fig. 1 Animal experiment scheme and design.

2.6. Oral glucose tolerance test (OGTT)

An oral glucose tolerance test was performed one week before the end of the intervention. Before testing, the mice were fasted overnight. The next day, after excision of about 1 mm of the tail tip of the mice using a scalpel, the fasting (t = 0 min) blood glucose concentration of the mice was detected by a handheld blood glucose meter (One Touch Ultra). This was followed by gavage of 20 wt% glucose solution at a dose of 2 g glucose per kg body weight, and the mouse blood glucose levels were detected at t = 15 min, 30 min, 60 min, 90 min, and 120 min after the end of gavage.[19] The OGTT curve was drawn according to the blood glucose values at different times, and the area under the blood glucose response curve (AUC) was calculated.

2.7. Biochemical analysis of serum

The total triglycerides (TG), total cholesterol (TC), low-density lipoprotein cholesterol (LDL-C) and high-density lipoprotein cholesterol (HDL-C) levels in the serum were determined using biochemical kit assays.

Fasting blood glucose (FBG) was measured using a handheld glucose meter, and fasting insulin (FINS) was measured using an ELISA kit. According to the FBG and FINS detection results, the steady-state assessment model was used to quantify the insulin resistance of the mice. For the homeostasis assessment model of insulin resistance index (HOMA-IR), the calculation formula is HOMA-IR = FBG ($mmol^{-1}$) × FINS ($mU\ L^{-1}$)/22.5.

Appetite-related hormones glucagon-likepeptide-1 (GLP-1), peptide YY (PYY) and leptin were determined by ELISA according to the operating instructions.

Serum inflammatory factors TNF-α, IL-6 and IL-1β were determined by ELISA kits according to the operating instructions.

2.8. Biochemical analysis of the liver

Liver tissue of no less than 50 mg was weighed and added to PBS homogenate with pH = 7.3 at a ratio of 1 g : 9 mL and then ground in a liquid nitrogen environment. Then, it was transferred to a centrifugal tube, centrifuged at 5000 rpm at 4 °C for 15 min, and the supernatant was taken to be measured. The activities of malondialdehyde (MDA), alanine aminotransferase (ALT) and aspartate aminotransferase (AST) in the livers of the mice were detected by biochemical kits.

2.9. Histological observation of the liver and fat

The epididymal fat and liver tissues were fixed with 4% paraformaldehyde, washed with tap water and ethanol, dehydrated, cleared, infiltrated with paraffin, then embedded in paraffin, cut into 4 μm sections, and stained with hematoxylin–eosin (HE) for morphological observation. The morphology was observed under an Olympus light microscope (Japan).

2.10. Genetic testing for glucose and lipid metabolism in the liver

Total RNA was extracted from the liver tissue using the Trizol method, its integrity was detected by agarose gel electrophoresis, and its purity was detected by a Nano-200 nucleic acid quantifier. According to the instructions for the reverse transcription kit (Takara PrimeScript RT Master Mix, Dalian, China), 1 mg of RNA was reversed to cDNA with a 9600 gene thermal cycler PCR machine. To detect target gene mRNA levels, real-time quantitative PCR was performed using the CFX 384 real-time system (Bio-Rad, Hercules, CA). The mouse-derived primers are shown in Table S2.† β-Actin was used as an internal control and $2^{-\Delta\Delta Ct}$ was used to calculate the relative gene expression.

2.11. Determination of fecal short-chain fatty acids

A Shimadzu GC-2010 Plus (Shimadzu, Japan) gas chromatograph was used to detect the content of short-chain fatty acids (SCFAs) in mouse feces. The determination method was described in a previous study.[20] The chromatographic column was an Agilent J&W DB-FFAP capillary column (30 m × 0.25 mm × 0.25 μm). The injection volume was 1 μL and the split ratio was 10 : 1. The initial temperature was 105 °C, which was raised to 170 °C at a rate of 10 °C min^{-1} and then raised to 230 °C at a rate of 20 °C min^{-1} and held for 2 min. Helium was used as the carrier gas at a flow rate of 1.0 mL min^{-1}. About 0.2 g of mouse feces was weighed, 1000 μL of ultrapure water was added, the sample was vortexed for 5 min and centrifuged at 14 000 rpm and 4 °C for 10 min, and the upper layer was filtered through a filter membrane to obtain 300 μL of supernatant. Then, 100 μL of 50% (v/v) concentrated sulfuric acid was added and mixed well. 300 μL diethyl ether was then added, and the sample was vortexed for 5 min, placed on ice for 5 min, and centrifuged at 14 000 rpm for 5 min at 4 °C. 200 μL of supernatant was taken into the inner cannula, sealed, and analyzed by the machine. The external standard method was used to quantify SCFAs. Table S3† shows the standard curve of mixed acids and the precision of instrument detection. The unit of SCFA in feces was μmol g^{-1}. Chromatographic grade SCFA standards were purchased from Shanghai Aladdin Biochemical Technology Co., Ltd (Shanghai, China).

2.12. Microbiota analysis

Total genomic DNA was extracted from stool samples using a DNA extraction kit (Omega Bio-tek, Norcross, GA, USA). The extracted DNA was subsequently quality-checked for concentration, purity, and integrity. Initial PCR amplification of the highly variable region V3–V4 of the bacterial 16S rRNA gene was performed, and amplicon PCR products were purified using the AxyPrep DNA Gel Extraction kit (AxyPrep Biosciences, Union City, CA, USA). Quantification was also performed using a Quantus fluorometer (Promega, Madison, WI, USA). Finally, amplicon sequencing was performed on an Illumina MiSeq PE300 platform (Illumina, San Diego, CA,

USA). The Majorbio cloud platform (https://cloud.majorbio.com) was used for bioinformatics analysis of intestinal flora.

2.13. Data analysis

All data are presented as mean ± SD unless otherwise stated. Origin 2023b was used for drawing, and IBM SPSS Statistics 26 was used for statistical analysis. After testing the data for normality and homogeneity of variance, one-way ANOVA was used to evaluate the treatment effect of each outcome, and Tukey's method was selected for *post hoc* analysis, with comparisons of means between groups and differences considered significant at $p < 0.05$.

3. Results and discussion

3.1. Infrared analysis

Infrared spectroscopy serves as an effective tool for analyzing molecular structure by detecting vibrations between atoms and molecular rotations.[21] The infrared absorption spectra of the KS, DK, KG and FKG samples exhibited similar characteristic peaks. All samples displayed an O–H stretching vibration peak at 3385 cm^{-1}, a C–H stretching vibration peak at 2902 cm^{-1},[22] and mannose characteristic absorption peaks at 879 cm^{-1} and 807 cm^{-1} (Fig. 2).[23] Notably, the KS sample showed a distinct absorption peak near 1735 cm^{-1}, indicative of a carbonyl group, suggesting the presence of acetyl groups in its molecular structure.[24] In contrast, the infrared spectra of DK, KG, and FKG lacked a peak near 1733 cm^{-1}, signifying the absence of acetyl groups in these samples. The presence of acetyl groups in the KGM molecules hinders the formation of intramolecular hydrogen bonds, facilitating interaction with water. Consequently, the hydration property of KGM is inversely related to the acetyl group content.[25]

3.2. Rheological analysis

The rheological properties of dietary fiber, particularly its viscosity, significantly influence its biochemical activity.[26] Consequently, the steady-state shear flow behavior of KS, DK, KG, and FKG (4 wt%) at 37 °C was examined. The findings demonstrated that all samples were pseudoplastic fluids exhibiting shear thinning, with KS showing the most pronounced effect due to its highest initial viscosity (Fig. 3). These observations are consistent with prior research on KGM sol and KGM gel.[27,28]

To more accurately investigate the flow behavior of KS, DK, KG and FKG, this study referred to other methods and fitted the steady-state shear data of the samples with the Williamson model.[29] The Williamson model expression is as follows:

$$\frac{\eta_a}{\eta_0} = \frac{1}{1+(\lambda w\gamma)^N} \cong \frac{1}{1+(\lambda w\gamma)^n}$$

η_a is the apparent viscosity (Pa s) of the fluid at any shear rate of γ (s^{-1}). η_0 is zero shear viscosity (Pa s), which is the theoretical apparent viscosity of the fluid at rest. λ_W is Williamson's time constant, expressed in s; $\lambda_W = 1/\gamma_c$, where γ_c (s^{-1}) is the critical shear rate of the sample; and n is the flow index.

Table 1 demonstrates that the fitting coefficients, R^2, for the Williamson equation all exceed 0.99, suggesting that this model is suitable for analyzing the steady-state flow behavior of KS, DK, KG, and FKG. Analyzing the zero-shear viscosity (η_0), KS exhibits a significantly higher η_0 compared to KG, with KG's η_0 being higher than FKG's, and FKG's higher than DK's. A shear rate of 50 s^{-1}, commonly associated with the forces generated by gastrointestinal peristalsis or oral chewing, is considered in evaluating the samples' behavior *in vivo*.[30] At this rate, the apparent viscosities (η_{50}) are as follows: KS

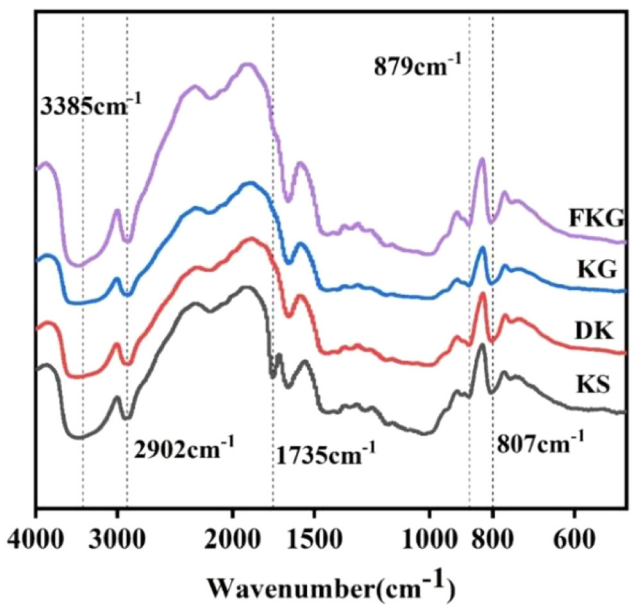

Fig. 2 FTIR spectra of KS, DK, KG, and FKG.

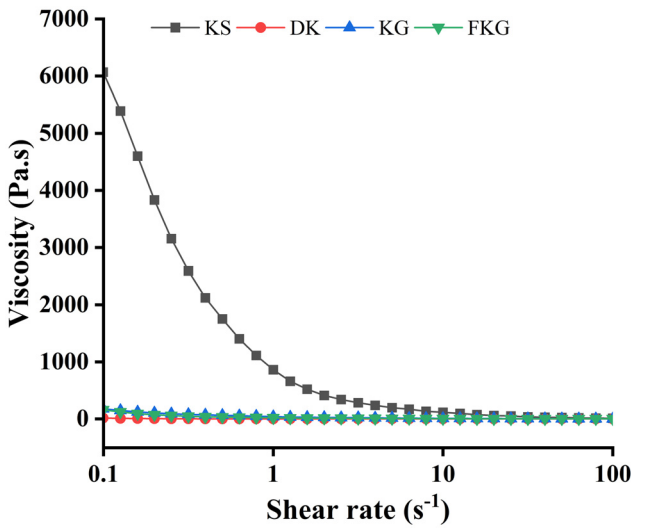

Fig. 3 Steady flow of KS, DK, KG, and FKG.

Table 1 Rheological properties of KS, DK, KG, and FKG

Group	η_0 (Pa s)	γ_c (s^{-1})	n	R^2	η_{50} (Pa s)
KS	10 488 ± 112^{d}	191.940 ± 10.225^{d}	0.910 ± 0.008^{c}	0.9977	18.940 ± 1.122^{c}
DK	132 ± 8^{a}	1.555 ± 0.543^{a}	0.915 ± 0.005^{c}	0.9984	0.008 ± 0.001^{a}
KG	2246 ± 105^{c}	39.658 ± 2.116^{b}	0.780 ± 0.010^{b}	0.9946	3.996 ± 0.032^{b}
FKG	1137 ± 87^{b}	131.004 ± 8.450^{c}	0.695 ± 0.006^{a}	0.9990	3.921 ± 0.047^{b}

Means with different lower-case letters within one column differed significantly between groups at $p < 0.05$.

Table 2 Effects of KS, DK, KG, and FKG on basic indicators of mice (n = 8)

Item	C	HF	KS	DK	KG	FKG
Initial body weight (g)	19.67 ± 1.07^{a}	19.63 ± 0.99^{a}	19.63 ± 0.90^{a}	19.63 ± 0.78^{a}	19.64 ± 0.72^{a}	19.63 ± 0.64^{a}
Final body weight (g)	26.25 ± 1.15^{a}	32.84 ± 1.63^{c}	28.96 ± 1.00^{b}	29.86 ± 1.89^{b}	29.86 ± 1.39^{b}	28.30 ± 1.73^{ab}
Body weight gain (g)	6.65 ± 1.10^{a}	13.49 ± 1.51^{c}	9.26 ± 1.05^{b}	10.23 ± 2.24^{b}	10.51 ± 1.44^{b}	8.69 ± 1.14^{ab}
Food intake (g per day)	2.33 ± 0.13^{a}	1.87 ± 0.11^{b}	1.91 ± 0.14^{b}	1.83 ± 0.12^{b}	1.90 ± 0.20^{b}	1.85 ± 0.18^{b}
Energy intake (kcal per day)	8.97 ± 0.50^{a}	10.29 ± 0.61^{b}	10.51 ± 0.67^{b}	10.07 ± 0.66^{b}	10.45 ± 0.50^{b}	10.18 ± 0.59^{b}
Liver weight (g)	0.82 ± 0.04^{a}	0.84 ± 0.06^{a}	0.84 ± 0.08^{a}	0.84 ± 0.06^{a}	0.88 ± 0.09^{a}	0.87 ± 0.11^{a}
Total fat (g)	0.75 ± 0.14^{a}	2.74 ± 0.73^{d}	1.57 ± 0.45^{c}	1.83 ± 0.53^{b}	1.88 ± 0.93^{b}	1.86 ± 0.97^{b}
Total fat g per 100 g BW	3.07 ± 0.42^{a}	8.31 ± 0.80^{d}	5.42 ± 0.82^{c}	6.10 ± 1.22^{b}	6.02 ± 2.40^{b}	6.3 ± 3.38^{b}
Hepatosomatic index	3.40 ± 0.16^{a}	2.76 ± 0.30^{c}	2.98 ± 0.24^{bc}	3.02 ± 0.28^{b}	2.94 ± 0.34^{b}	2.73 ± 1.05^{b}
Lee's index	3.21 ± 0.16^{a}	3.52 ± 0.21^{b}	3.17 ± 0.17^{a}	3.29 ± 0.18^{a}	3.24 ± 0.18^{a}	3.17 ± 0.09^{a}

Means with different lower-case letter within one row differed significantly between groups at $p < 0.05$.

demonstrates the highest η_{50} at 18.9401 Pa s; KG and FKG show similar values of 3.9957 Pa s and 3.9208 Pa s, respectively; and DK exhibits the lowest, almost negligible, at approximately 0 Pa s. Given that high viscosity can enhance satiety by increasing the viscosity of the food substrate,[31] KS, with its higher η_0 and η_{50}, may be more effective in promoting satiety.

3.3. Macrophysiological evaluation

During the 12-week experiment, the mice consistently gained weight and maintained good mental health, suggesting no adverse effects from the experiment (Table S4†). Table 2 shows that there were no significant differences in body weight among the groups prior to dietary intervention. However, post-intervention, significant disparities in body weight emerged among the groups. By the experiment's conclusion, the average body weight in the high-fat diet group (HF) was 32.84 g, significantly exceeding that of the low-fat control group (C) ($p < 0.05$). Compared to the HF group, the KS, DK, KG, and FKG groups, which had the same energy density as HF, exhibited significantly reduced body weight and weight gain ($p < 0.05$). This indicates that the intake of KS, DK, KG, and FKG effectively mitigated rapid weight gain induced by a high-fat diet. Nonetheless, no significant differences were noted between the KS, DK, KG, and FKG groups.

Dietary fiber can boost satiety, suppress hunger, regulate energy intake, and ultimately aid in weight management.[32] In this study, the daily feed intake of the HF, KS, DK, KG, and FKG groups was significantly lower than that of the control group C, yet the average daily energy intake exhibited the opposite trend. No significant differences were observed in daily feed intake and energy intake between the KS, DK, KG, FKG, and HF groups ($p > 0.05$). This indicates that the resistance of KGM to rapid weight gain is not due to a reduction in food intake, but rather through decreased energy absorption and utilization and increased energy expenditure.[33,34] Similar findings were observed in some animal experiments, where KGM intake did not lessen food consumption in mice on a high-fat diet but increased the excretion of fats and bile acids in feces.

Body fat percentage and fat weight are often utilized as direct indicators to assess body obesity.[35] After 12 weeks of dietary intervention, the fat weights for the control, high-fat, KS, DK, KG, and FKG groups were 0.75 g, 2.74 g, 1.57 g, 1.83 g, 1.88 g, and 1.86 g, respectively. This data indicates that a long-term high-fat diet significantly increases the total adipose tissue in mice. Consumption of KS, DK, KG, and FKG reduced the total adipose tissue weight in mice fed a high-fat diet, although these reductions were not significantly different between the KS, DK, KG, and FKG groups. The trend in body fat percentage paralleled that of fat weight. Additionally, analysis of the liver weights in each group revealed that despite the increase in body weight from the high-fat diet, there was no significant increase in liver weight, suggesting that the level of obesity induced by the high-fat diet in this study was insufficient to affect liver mass in mice.

Lee's index is widely used for assessing obesity in mice, analogous to the body mass index (BMI) used in human studies.[36] Generally, a higher Lee's index suggests greater obesity. According to Table 2, the Lee's index for the HF group was significantly higher than that of other groups ($p < 0.05$). However, no significant differences were observed between the KS, DK, KG, FKG, and C groups ($p > 0.05$).

3.4. Histological observation of liver and fat

Pathological examination of the mouse liver revealed that hepatocytes in group C were typically polygonal and neatly arranged, and displayed a regular, radial configuration around the veins. In contrast, hepatocytes in the HF group appeared swollen, with numerous large adipose vacuoles. This suggests that a long-term high-fat diet significantly disrupts normal lipid metabolism in the mouse liver, leading to excessive lipid accumulation within hepatocytes. In the liver tissues of the KS, DK, KG, and FKG groups, while some fat vacuoles and cellular enlargement and proliferation were evident, the overall cellular structure remained relatively normal. This indicates that the ingestion of four typical konjac dietary fibers may mitigate fat accumulation, ameliorate liver fat deformation, and thus maintain stable liver cell morphology, as shown in Fig. 4.

The cell morphology of adipose tissue reflects the impact of treatments with KS, DK, KG, and FKG on obesity. Adipose tissue cells in the control group (C) were small, uniformly shaped, structurally intact, and densely packed.[37] In contrast, cells in the high-fat (HF) group were larger and irregular in shape. However, the adipocyte morphology in the KS, DK, KG, and FKG groups showed significant improvements compared to the HF group. Although some cells remained enlarged, the adipocytes in these treatment groups were uniform, regular, and densely arranged, akin to those in the control group. This suggests that dietary intake of KS, DK, KG, and FKG can partially inhibit fat accumulation in the adipose tissue of mouse epididymis, with KS, KG, and FKG showing a greater inhibitory effect than DK (Fig. 5).

3.5. Effects of KS, DK, KG and FKG on glucose regulation

The OGTT experiment was conducted in the 12th week of dietary intervention to assess the impact of a long-term high-fat diet on insulin sensitivity in mice. As depicted in Fig. 6A–E, prolonged high-fat diet exposure appears to disrupt the glucose regulatory balance in HF group. During the 2 h metabolic assessment, blood glucose levels in the HF group remained at a high level. Blood glucose peaked at 15 min post-gavage in all groups, with the HF group exhibiting significantly higher levels compared to the C and KS groups. Meanwhile, the peak values in the DK, KG, and FKG groups were comparable to that of the HF group. After 2 h, blood glucose in the HF group decreased slightly but remained substantially above baseline, whereas levels in the KS, KG, and FKG groups returned to normal, akin to the C group. However, levels in the DK group continued to mirror those in the HF group throughout the 2 h period. Fig. 6B illustrates that the AUC for the HF group during this period was significantly greater than that of the C group, showing a 20.92% increase ($p < 0.05$). After 12 weeks of KS dietary intervention, the AUC of the KS group returned to the normal level. Although the blood glucose levels of KG and FKG at 120 min were significantly lower than those of the HF group, the blood glucose level in the first 90 min during the OGTT process could not significantly reduce the high blood glucose level induced by high-fat diet. Therefore, the average AUC of the final OGTT area in KG and FKG was slightly lower than that of the HF group with no significant difference ($p > 0.05$).

The fasting blood glucose levels of mice in each group were further analyzed as shown in Fig. 6C. The values for groups C, HF, KS, DK, KG, and FKG were 6.2 mmol L^{-1}, 7.3 mmol L^{-1}, 6.4 mmol L^{-1}, 7.0 mmol L^{-1}, 6.8 mmol L^{-1}, and 6.6 mmol L^{-1}, respectively. Compared to group C, fasting blood glucose (FBG) in the HF group increased by 17.74%. The FBG levels in the KS and FKG groups were significantly reduced by 12.33% and 9.59%, respectively, compared to the HF group, whereas

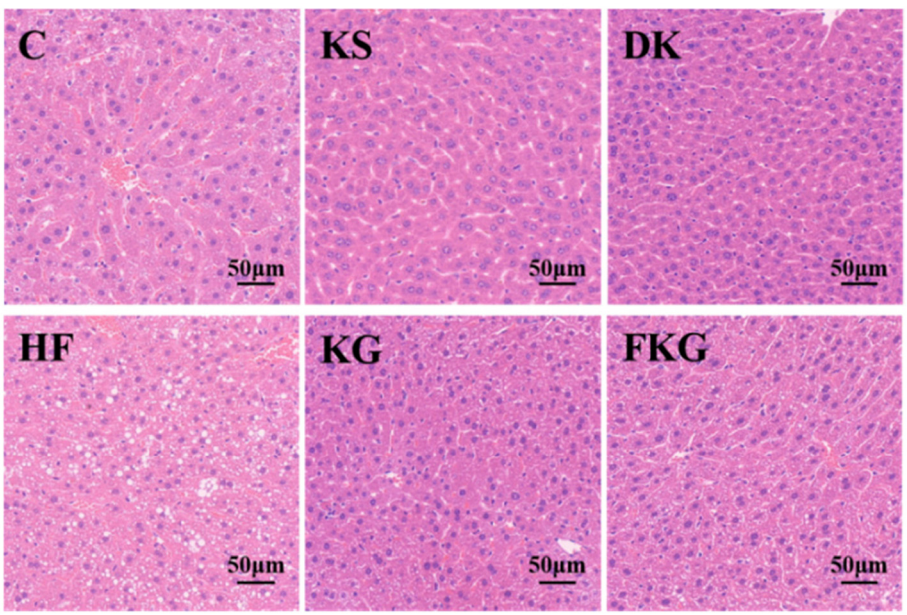

Fig. 4 Histopathological observation of the liver tissue stained with H & E.

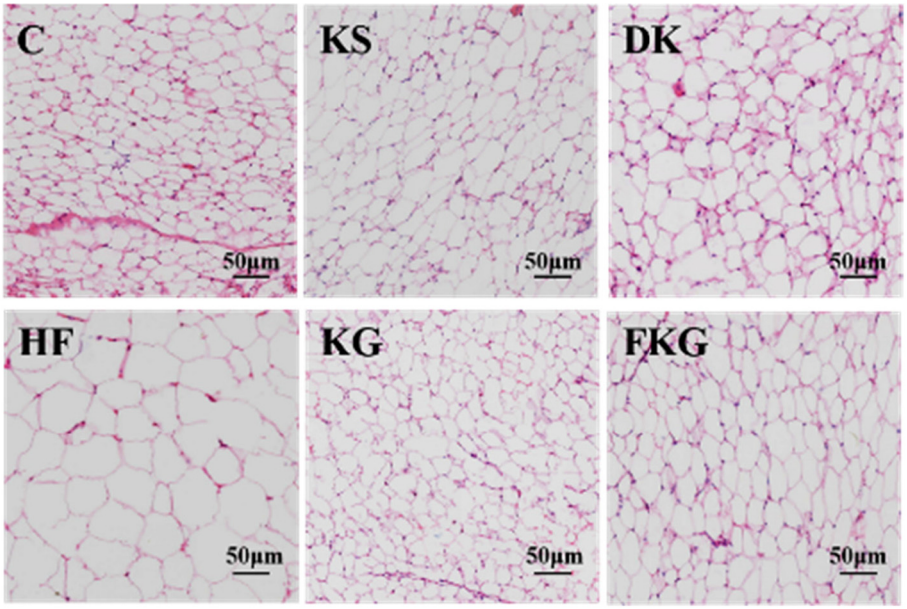

Fig. 5 Histopathological observation of the abdominal fat tissue stained with H & E.

the mean FBG values in the DK and KG groups were marginally lower than those in the HF group but without a significant difference ($p > 0.05$). Further analysis of the insulin levels is presented in Fig. 6D. The fasting insulin levels in groups C, HF, KS, DK, KG, and FKG were 10.30 mIU L^{-1}, 13.06 mIU L^{-1}, 9.98 mIU L^{-1}, 10.41 mIU L^{-1}, 11.25 mIU L^{-1}, and 10.69 mIU L^{-1}, respectively. The fasting insulin level in the HF group was 26.80% higher compared to group C. Relative to the HF group, the KS group showed a 23.58% decrease in fasting insulin levels, while the DK, KG, and FKG groups exhibited reductions of 20.29%, 13.86%, and 18.15%, respectively. The high-fat diet led to reduced insulin sensitivity in the mice; however, this effect was significantly ameliorated by the KS, DK, KG, and FKG samples.

Fig. 6E presents the HOMA-IR of the mice in each group. Mice in the HF group exhibited a significantly higher insulin resistance index compared to those in the other groups, although no significant differences were observed between the KS group and the C group. The insulin resistance indices of the mice in the DK, KG, and FKG groups were significantly lower than that of the HF group, with no significant differences among these three groups.

3.6. Effects of KS, DK, KG and FKG on appetite regulation

A high-fat diet reduced the baseline levels of GLP-1 and PYY in mice, which were significantly lower than those observed in the control group ($p < 0.05$). Subsequent analysis indicated that KS intake elevated the baseline GLP-1 and PYY levels in mice fed a high-fat diet (Fig. 7). FKG consumption also increased the serum GLP-1 levels in these mice but did not significantly affect the serum PYY levels ($p > 0.05$). Conversely, DK and KG intake did not enhance the serum GLP-1 or PYY levels in the mice on a high-fat diet. The serum leptin levels were not significantly different among the C, HF, KS, and KG groups ($p > 0.05$); however, they were higher in the DK group compared to the KS and KG groups, while the leptin levels in the FKG group were significantly lower than those in the KS and KG groups ($p < 0.05$).

3.7. Effects of KS, DK, KG and FKG on lipid metabolism

The role of KGM in maintaining lipid homeostasis has attracted considerable attention.[38–40] Accordingly, this study evaluated the hypolipidemic effects of the four types of konjac dietary fiber. As illustrated in Fig. 8, a high-fat diet elevated the serum levels of TG, TC, and LDL-C while significantly reducing HDL-C levels ($p < 0.05$). Compared to control group C, the HF group exhibited increases of 85.37% in TG, 48.51% in TC, and 166.67% in LDL-C, along with a 32.37% reduction in HDL-C. Relative to the HF group, the intake of KS, DK, KG, and FKG significantly ameliorated the blood lipid levels in mice; the serum TG and TC levels in these groups were notably lower than those in the HF group ($p < 0.05$). Further comparison of the hypolipidemic effects of KS, DK, KG, and FKG revealed that all samples mitigated the rise in serum TG and TC levels induced by a high-fat diet, although no significant differences were observed in the TG and TC reduction capabilities among the four samples ($p > 0.05$). Regarding the LDL-C and HDL-C levels in serum, KS was more effective at improving blood lipid profiles than DK, KG, and FKG, with no significant differences noted between FKG, DK, and KG ($p > 0.05$).

3.8. Effects of KS, DK, KG and FKG on liver biomarkers

Oxidative stress is a critical indicator of obesity, with malondialdehyde (MDA) serving as a biomarker for this condition.[41] Thus, assessing MDA levels in the body can reflect the extent of oxidative cell damage.[42] Fig. 9A displays the MDA levels in

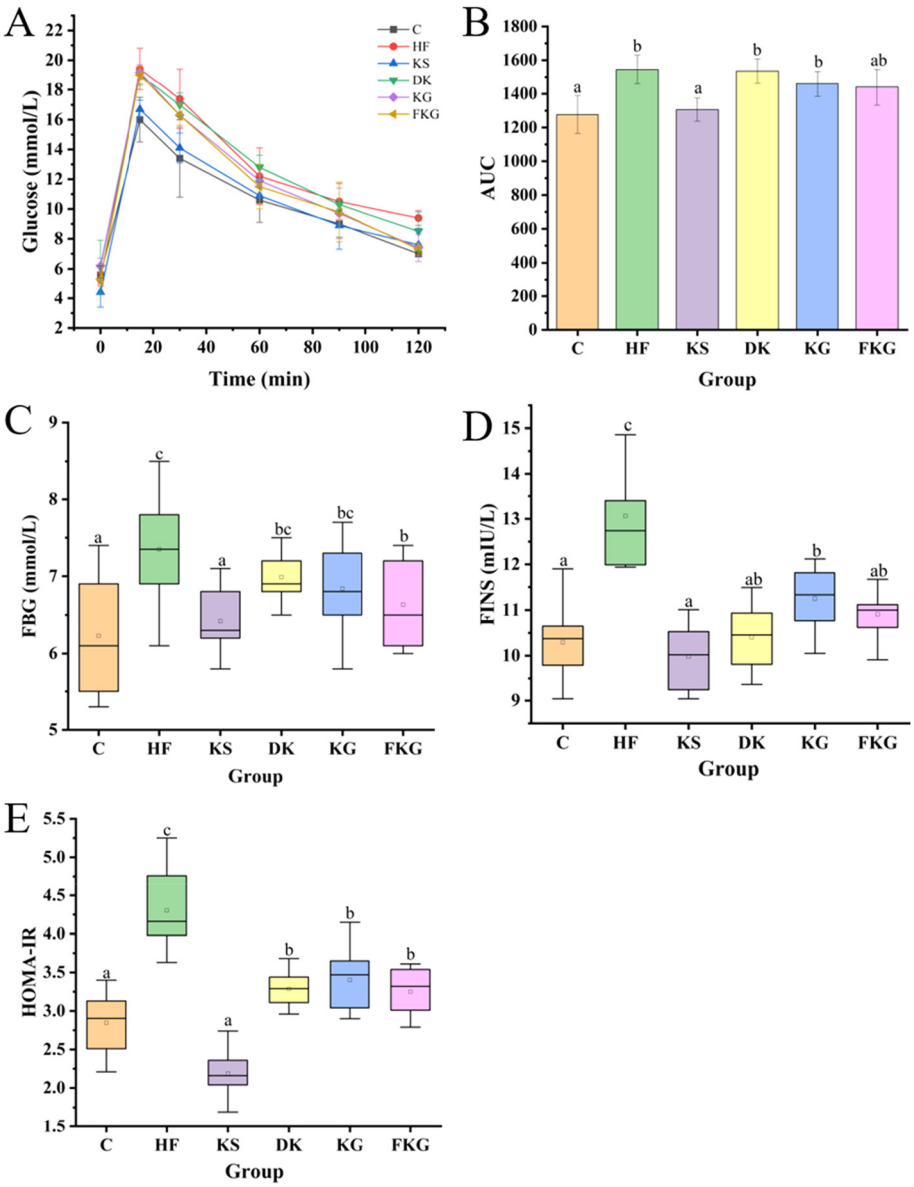

Fig. 6 Analysis of the OGTT (A), AUC (B), FBG (C), FINS (D) and HOMA-IR (E) of the mice (n = 8).

the liver of mice across groups. A high-fat diet exacerbated lipid peroxidation, leading to increased MDA levels in the liver. Compared to the high-fat (HF) group, the MDA levels in the liver of the KS, DK, KG, and FKG groups were significantly reduced ($p < 0.05$).

Individuals who are overweight or obese are at an elevated risk of developing steatosis, potentially leading to impaired liver function.[43] Liver enzymes, alanine aminotransferase (ALT), and aspartate aminotransferase (AST), are commonly utilized as biomarkers of liver injury due to their high specificity and sensitivity.[44] This study aimed to examine the direct effects of a prolonged high-fat diet on mouse liver by analyzing AST and ALT levels. Fig. 9B and C illustrate that a long-term high-fat diet inflicted considerable liver damage, as evidenced by the significant increase in AST and ALT levels in the liver of the high-fat (HF) group. Conversely, the addition of konjac glucomannan (KGM) markedly ameliorated the liver damage induced by the high-fat diet. The experimental results revealed that the AST and ALT levels in the livers of the konjac-supplemented (KS), diacylglycerol-enriched (DK), konjac glucomannan (KG), and fiber-enriched konjac glucomannan (FKG) groups were significantly lower than those in the HF group ($p < 0.05$). This protective effect is primarily attributed to the reduction in excessive lipid absorption and the consequent alleviation of the metabolic burden on the liver by these interventions.

3.9. Effects of KS, DK, KG and FKG on serum inflammatory cytokines

As illustrated in Fig. 10, a high-fat diet significantly elevated the serum levels of TNF-α, IL-1β, and IL-6. However, the consumption

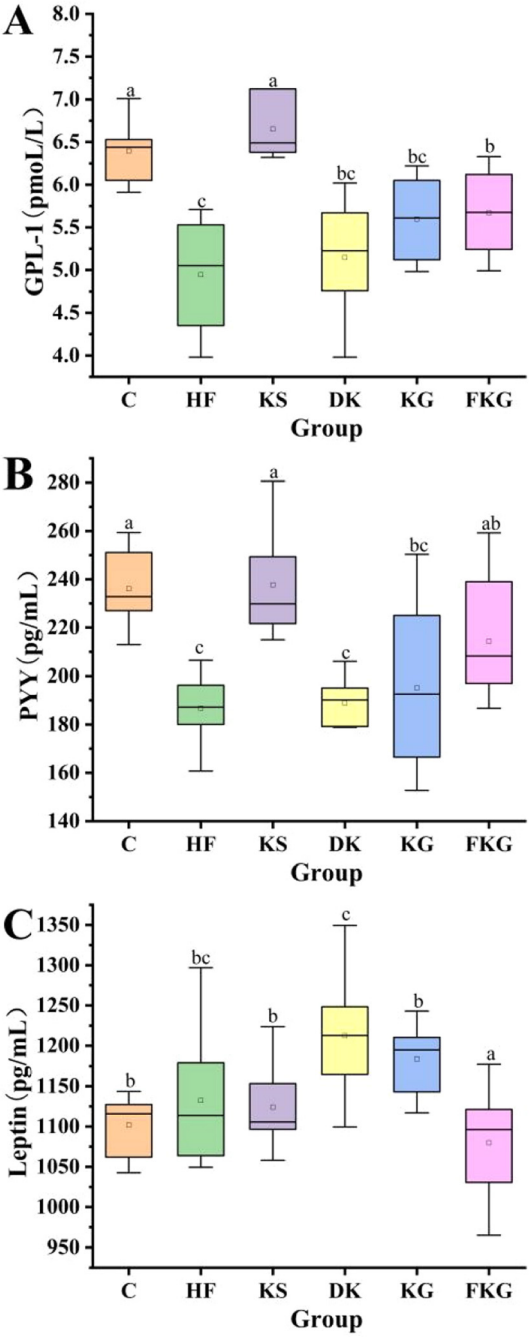

Fig. 7 The content of appetite hormones GLP-1 (A), PYY (B) and leptin (C) in mice during the fasting state (n = 8).

of four types of konjac dietary fiber—KS, DK, KG, and FKG—effectively attenuated the inflammatory response. There were no significant differences in the levels of inflammatory markers among the KS, DK, KG, and FKG groups ($p > 0.05$).

3.10. Effects KS, DK, KG and FKG on the genes of glucose and lipid metabolism

Compared to the HF group, the expression level of the *GCK* gene in the C group was reduced to 0.31 times, while the expression level of the *GSK-3β* gene remained consistent with that in the HF group. Moreover, the expression levels of the *G-6-pase* gene and *PEPCK* mRNA were increased by 0.97 and 1.22 times, respectively. The expression level of *Glut4* mRNA in the C group was elevated to 2.01 times. This study indicates that a high-fat diet reduces the expression levels of *G-6-pase*, *PEPCK*, and *Glut4* mRNA while increasing the expression of *GCK* mRNA. Compared to the HF group, the expression level of *GCK* mRNA in the KS, DK, KG, and FKG groups was decreased, and the expression levels of *GSK-3β* mRNA, *G-6-pase* mRNA, *PEPCK* mRNA, and *Glut4* mRNA were elevated. The influence of DK, KG, and FKG on the expression of genes related to glucose metabolism was similar; however, KG and FKG, unlike KS, could significantly increase the expression levels of *GCK* and *G-6-pase* mRNA compared to DK (Fig. 11).

In terms of liver lipid metabolism, KS, DK, KG, and FKG influenced several lipid metabolism-related genes similarly to those in the HF group. They all up-regulated the expression of *LDLR*, *SR-B1*, *CYP7A1*, and *PPARα* mRNA while down-regulating the expression of *FXR* mRNA. There were no significant differences in the expression of *SR-B1*, *CYP7A1*, *FXR*, and *PPARα* among KS, DK, KG, and FKG ($p > 0.05$), except that *LDLR* exhibited a higher expression level in KS (Fig. 12).

3.11. Effects of KS, DK, KG and FKG on SCFA determination

There was no significant difference in the acetic acid content in the feces of all groups except the KS group, which exhibited a significantly higher acetic acid content compared to the other groups. Analysis of the propionic acid content among the groups revealed that a high-fat diet notably decreased fecal propionic acid levels in comparison to group C. However, dietary intervention with KS ameliorated this effect, as evidenced by the significantly higher fecal propionic acid content in the KS group compared to the HF group. The levels of propionic acid in the DK, KG, and FKG groups were similar to those in the HF group. Additionally, the contents of isobutyric acid and butyric acid across all groups mirrored the trends observed in propionic acid. Examination of the isovaleric and valeric acid contents in each group indicated that KS and DK significantly elevated these acids in high-fat diet mice. Regarding total acid content, KS and DK interventions markedly increased the total fecal SCFA content. Notably, the total SCFA content in the DK group returned to normal levels, whereas in the KS group, it surpassed that of the normal control group. The total fecal SCFA levels in the KG and FKG groups were slightly higher than that in the HF group, albeit without significant difference. This suggests that a high-fat diet primarily reduces the fecal content of propionic acid, isobutyric acid, and butyric acid. Further analysis of the SCFA content in mice fed four types of konjac dietary fiber revealed that the KS group experienced the greatest increase in SCFA content, while DK predominantly augmented the isovaleric acid content. KG and FKG did not significantly alter the SCFA levels in the feces of high-fat diet mice (Fig. 13).

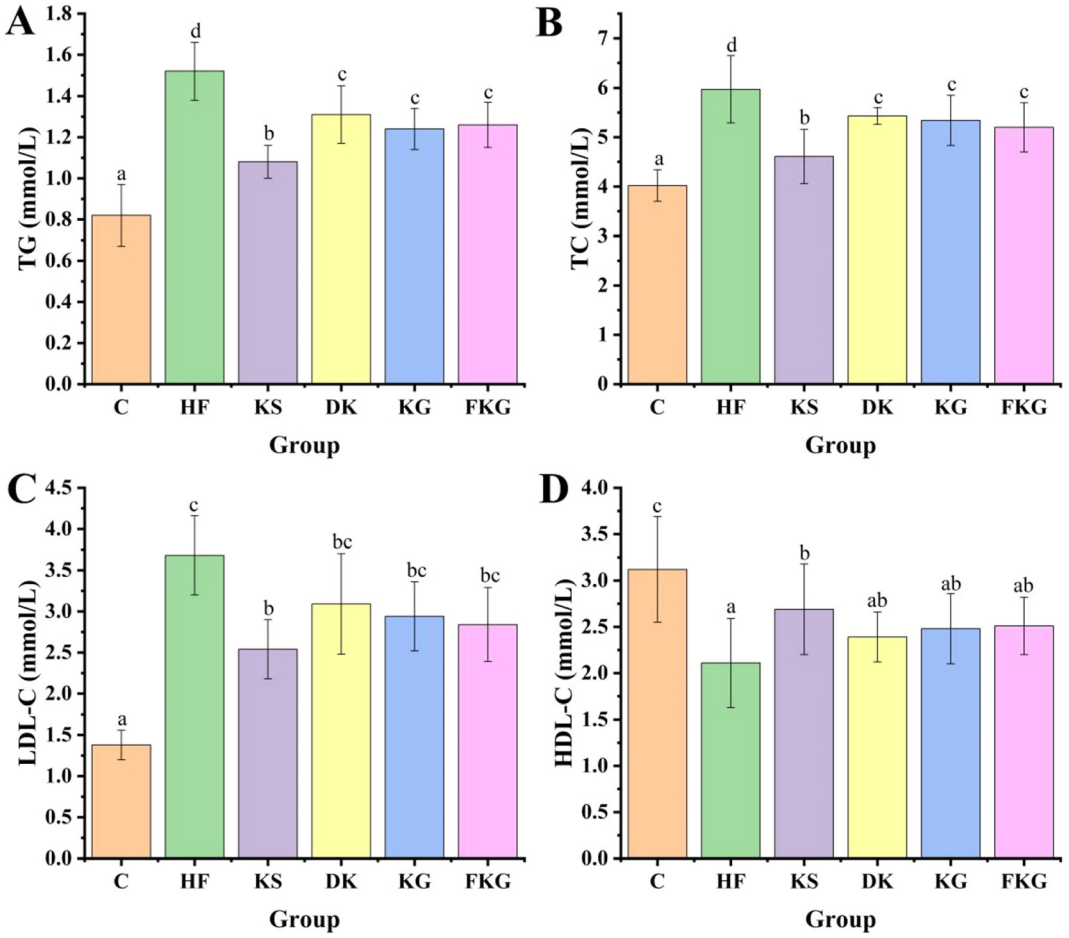

Fig. 8 Effects of KS, DK, KG and FKG on the serum lipid levels of TG (A), TC (B), HDL-C (C) and HDL-C (D) in mice (n = 8).

3.12 Effects of KS, DK, KG and FKG on intestinal flora

There were 132 operational taxonomic units (OTUs) across the C, HF, KS, DK, KG, and FKG groups. Specifically, the unique OTUs in the C, HF, KS, DK, KG, and FKG groups numbered 47, 9, 17, 40, 19, and 20, respectively, suggesting that a high-fat diet reduced the number of unique OTUs in the intestinal flora of mice. Intervention with KS, DK, KG, and FKG increased the count of unique OTUs. Further analysis revealed that the KG, FKG, and DK groups exhibited a higher number of unique OTUs and shared more OTUs with group C compared to the KS group (Fig. 14A). α-Diversity analysis corroborated these findings.

Principal Component Analysis (PCoA) revealed that samples from group C clustered together, while those from group HF were distinctly separated along the PCoA axis. Samples from the KS, DK, KG, and FKG groups were positioned on the left side of the axis, closely grouped with C and distinctly separate from samples from the HF group. In the non-metric multidimensional scaling (NMDS) diagram (Fig. S1†), samples within each group—C, HF, KS, DK, KG, and FKG—formed distinct clusters. Notably, groups C, KS, DK, KG, and FKG were clearly separated from group HF, corroborating the PCoA findings. This separation indicates significant differences in intestinal microbiota structure between the high-fat, low-fat, and four types of konjac dietary fiber groups. The inclusion of KS, DK, KG, and FKG in the diet countered the β diversity changes in mouse microflora induced by a high-fat diet. The continuous consumption of these four konjac diets improved the intestinal flora of mice, leading to a new homeostasis (Fig. 14B).

Compared to group C, the Chao1 and Shannon indices in the HF group were significantly decreased, while the Simpson index was significantly increased ($p < 0.05$). These α-diversity results suggest that HF diminishes intestinal microbial diversity, leading to microbial flora disorder. Conversely, the Chao1 (Fig. 14C) and Shannon (Fig. 14D) indices in the KS, DK, KG, and FKG groups were significantly higher than those in the HF group, while the Simpson index (Fig. 14E) was lower. This implies that the four types of konjac dietary fiber can effectively counteract the reduction in intestinal flora diversity caused by the HF and are beneficial for maintaining intestinal flora homeostasis. However, there were no significant differences in intestinal flora α diversity between the KS, DK, KG, and FKG groups.

The relative abundances of *Firmicutes* in the C, HF, KS, DK, KG, and FKG groups were 85.33%, 77.10%, 89.93%, 87.92%,

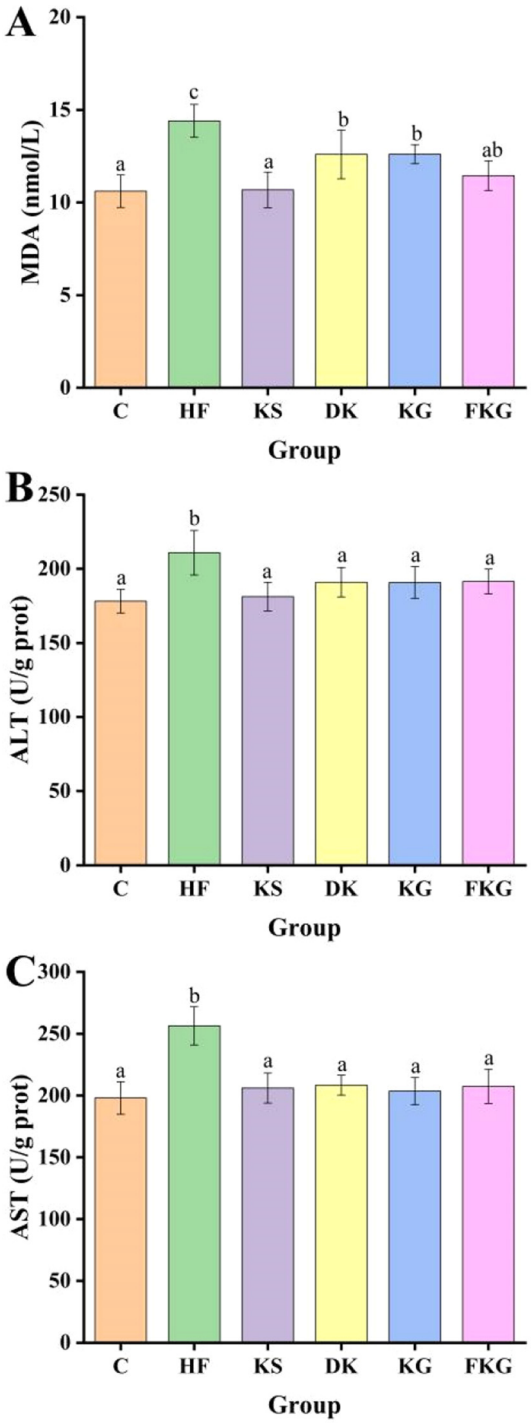

Fig. 9 Liver damage in mice. (A) AST, (B) ALT and (C) MDA levels.

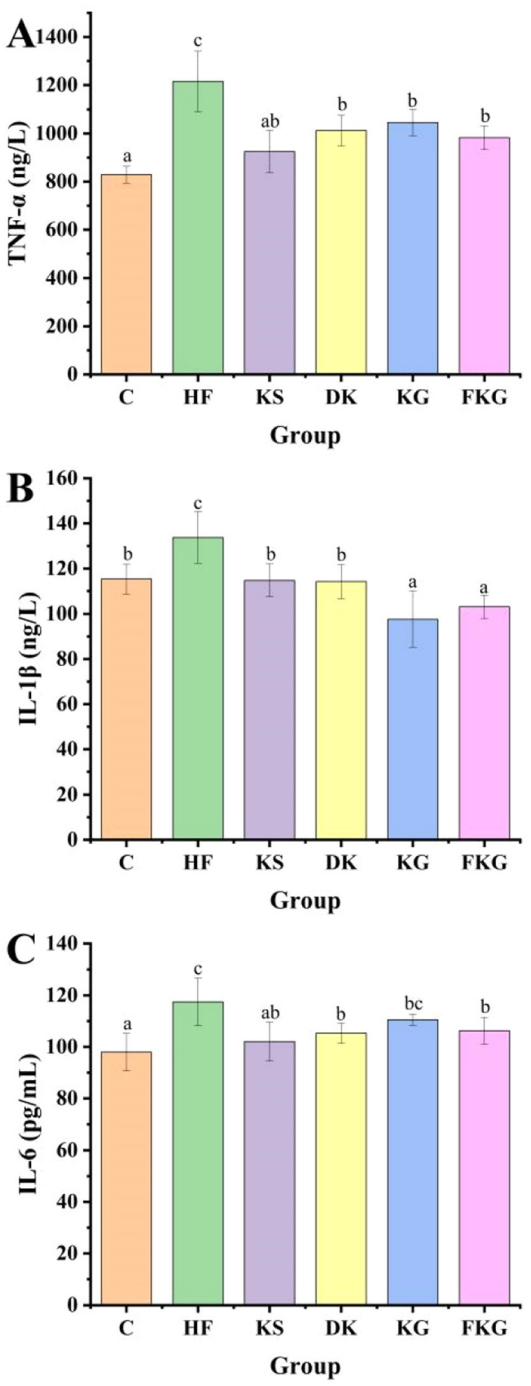

Fig. 10 Serum levels of inflammatory cytokines TNF-α (A), IL-1β (B), and IL-6 (C) in mice (n = 8).

90.54%, and 91.65%, respectively. Correspondingly, the relative abundances of *Bacteroidetes* were 9.77%, 19.32%, 6.57%, 8.35%, 5.00%, and 3.97%, respectively. A high-fat diet notably increased the abundance of *Bacteroidetes* while decreasing that of *Firmicutes*. Both human and animal studies have indicated that the ratio of *Firmicutes* to *Bacteroidetes* (*F*/*B* ratio) or *Bacteroidetes* to *Firmicutes* (*B*/*F* ratio) serves as a measure of gut microbiome health.[45] In this study, a high-fat diet reduced the *F*/*B* ratio of the intestinal flora. Conversely, the KS, DK, KG, and FKG treatments all enhanced the *F*/*B* ratio, aligning with findings from Duan *et al.*[46]

Species composition at the genus classification level revealed that the HF diet increased the abundance of *norank_f_Muribaculaceae*, *Faecalibaculum*, and *Lactobacillus* compared with group C, while it reduced the abundance of *Blautia*, *Romboutsia*,

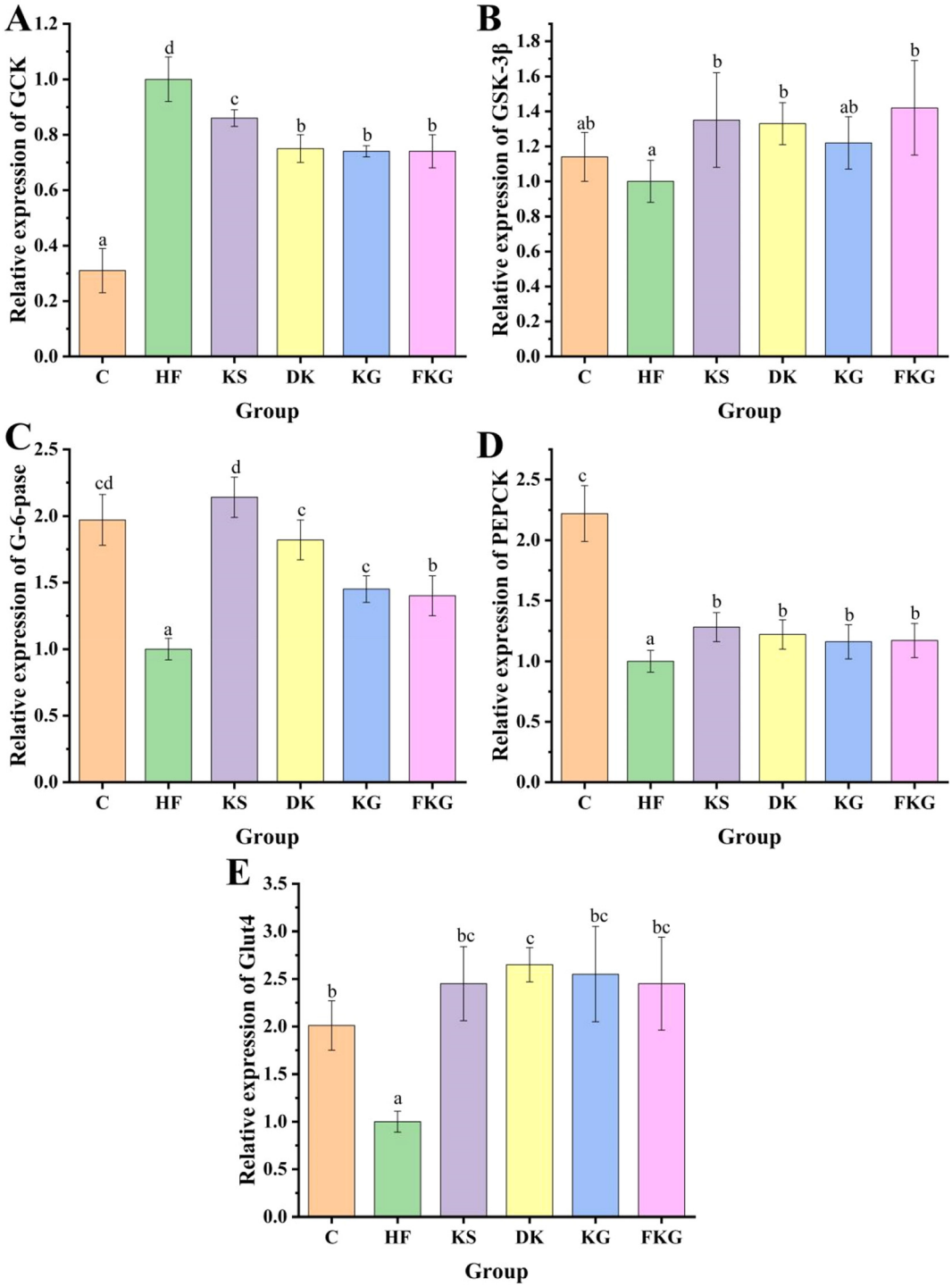

Fig. 11 Effects of KS, DK, KG and FKG on the mRNA expression of liver glucose metabolism genes *GCK* (A), *GSK-3β* (B), *G-6-pase* (C), *PEPCK* (D) and *Glut4* (E) in mice (n = 8).

Lachnospiraceae_NK4A136_group, *norank_f_Lachnospiraceae*, *Colidextribacter*, *unclassified_f_Lachnospiraceae*, and *norank_f_Oscillospiraceae*. In contrast, the KS intake, when compared with the HF group, decreased the abundance of *Faecalibaculum*, *Lactobacillus*, and *norank_f_Muribaculaceae* but increased the abundance of *Blautia*, *Colidextribacter*, *unclassified_f_Lachnospiraceae*, *norank_f_Lachnospiraceae*, *norank_f_Oscillospiraceae*, and *Lachnospiraceae_NK4A136_group*. Additionally, the inclusion of DK, KG, and FKG in the diet, as compared to the HF group, elevated the presence of *unclassified_f_Lachnospiraceae*, *norank_f_Lachnospiraceae*, *Blautia*, *Romboutsia*, *Colidextribacter*, *norank_f_Oscillospiraceae*, and *Lachnospiraceae_NK4A136_group* but diminished the abun-

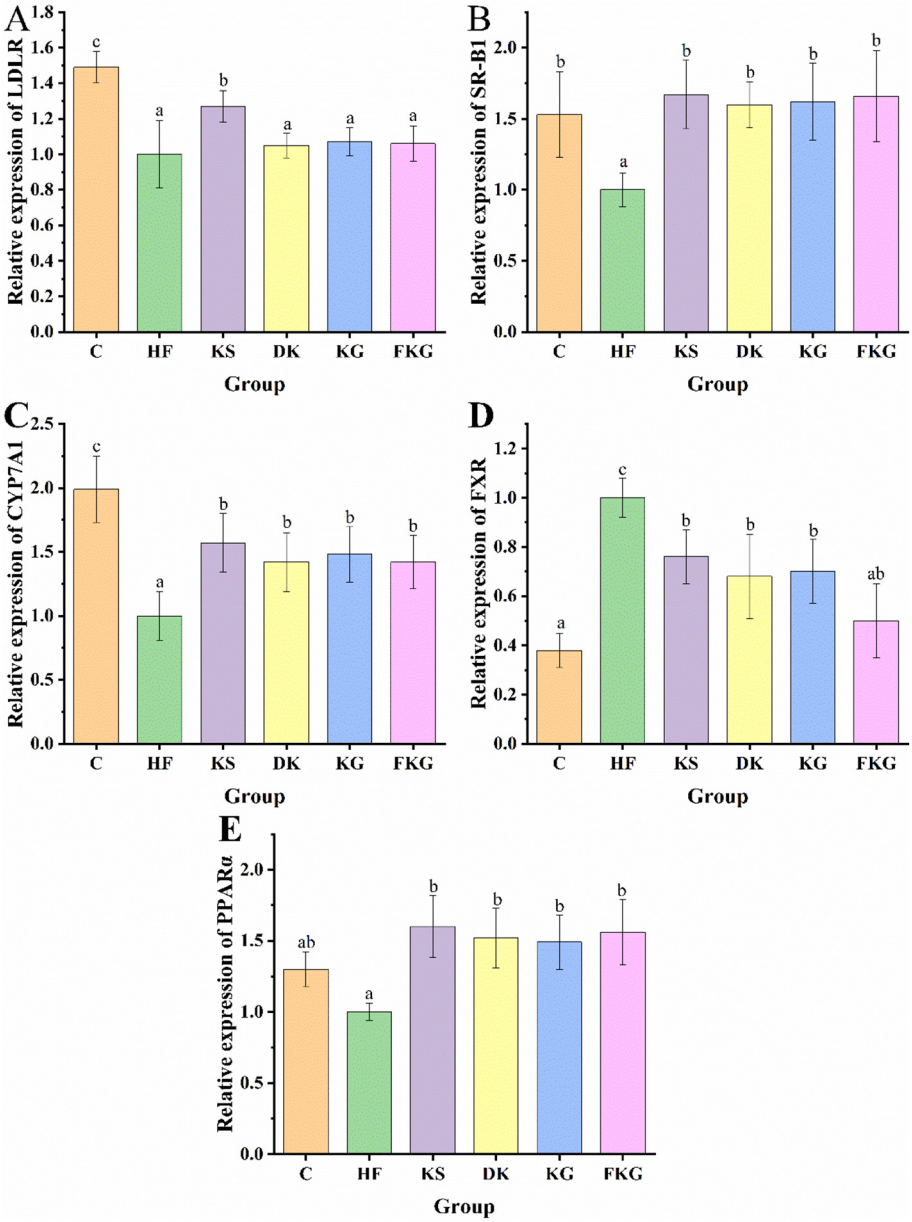

Fig. 12 Effects of KS, DK, KG and FKG on the mRNA expression of liver lipid metabolism genes *LDLR* (A), *SR-B1* (B), *CYP7A1* (C), *FXR* (D) and *PPARα* (E) in mice (n = 8).

dance of *Faecalibaculum* and *norank_f_Muribaculaceae*. Relative to the HF and C groups, the abundance of *Lachnospiraceae_NK4A136_group* in the KS, DK, KG and FKG groups was notably higher. *Romboutsia* was more readily enriched in the DK, KG, and FKG groups compared to the KS group, while *Blautia* was more enriched in the KS group. The bacterial composition in the KG and FKG groups was essentially similar, suggesting that the freezing treatment had minimal impact on the prebiotic activity of DK in this study; however, the abundance of *Lactobacillus* in the KG group exceeded that in the other five groups. Compared with KG, DK more effectively supported the growth of *Romboutsia* and *unclassified_f_Lachnospiraceae*, whereas KG favored the enrichment of *Faecalibaculum* and *Lactobacillus*.

In a prior study involving HFD-fed mice, a marked decline in the abundance of *Faecalibaculum* was observed, accompanied by reduced serum levels of pro-inflammatory cytokines and lipopolysaccharide-binding protein (LBP). This suggests its involvement in a pro-inflammatory pathway within the gut that is associated with metabolic disorders.[47] Among the KS, DK, KG, and FKG groups, the DK group exhibited the lowest *Faecalibaculum* abundance, which may be attributed to the low viscosity characteristic of the DK.

The genus *Blautia* has been identified as a symbiotic bacterium negatively associated with obesity and type 2 diabetes.[48] Oral administration of *Blautia wexlerae* in mice induced metabolic changes and anti-inflammatory effects, which in turn reduced obesity and diabetes caused by a high-fat diet. A

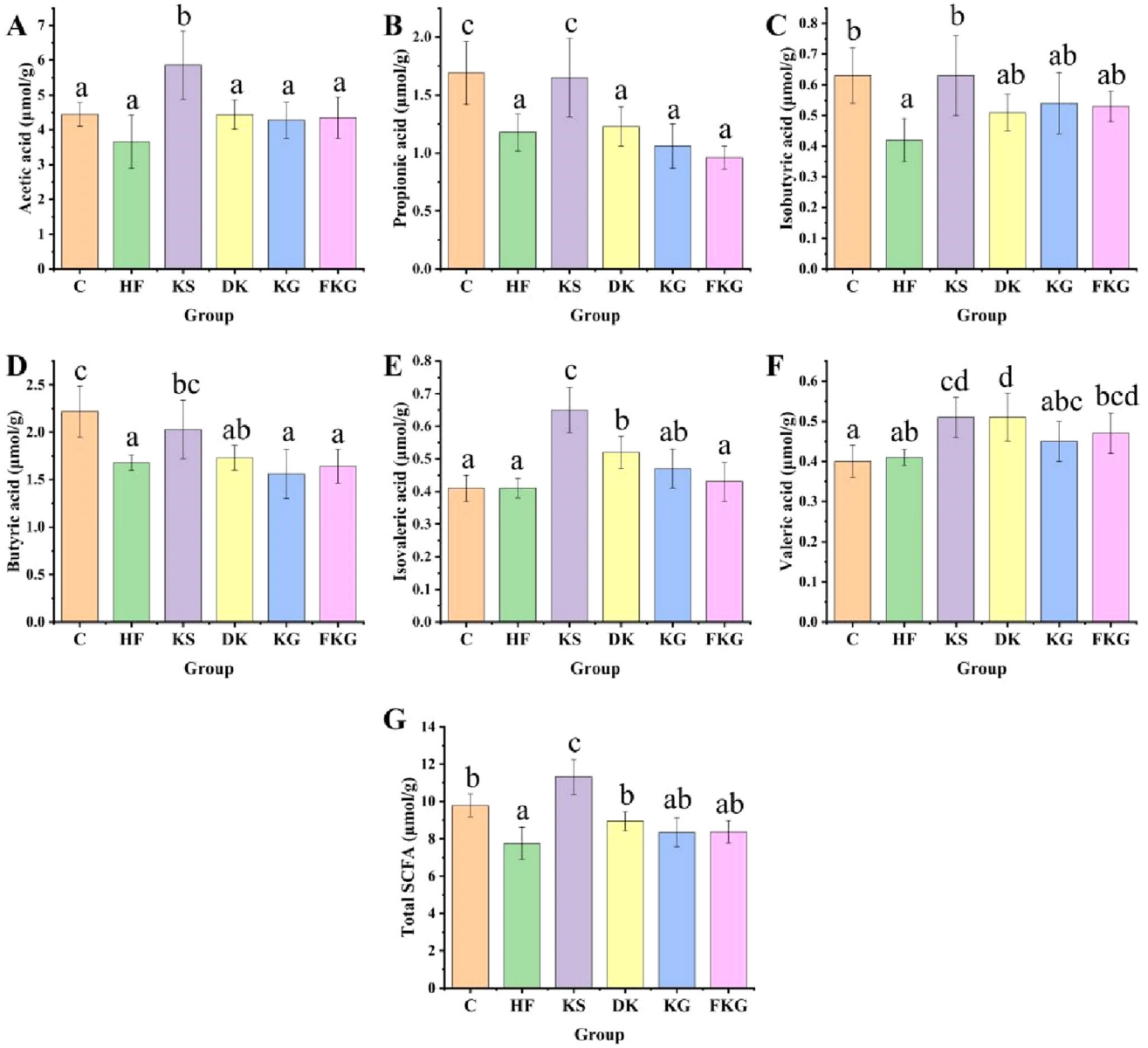

Fig. 13 The contents of short-chain fatty acids acetic acid (A), propionic acid (B), isobutyric acid (C), butyric acid (D), isovaleric acid (E), valeric acid (F), and total acid (G) in mice feces (n = 8).

similar phenomenon was observed in this study, where the abundance of *Blautia* in the HF group was significantly lower compared to those in the other five groups. KS, DK, KG, and FKG treatments notably increased the abundance of *Blautia*, with KS showing the greatest increase.

3.13. Correlation analysis

Dysbiosis of the gut microbiota can be caused by a combination of genetic and environmental factors. It has the potential to enhance energy absorption by altering gene expression and leading to excessive accumulation of short-chain fatty acids (SCFAs). Dysbiosis also influences central appetite through various mechanisms, such as the gut–brain axis, gut hormones, and neuromodulators. Additionally, it can regulate fat storage through transcription factors and lipoprotein lipase activity. Furthermore, it may contribute to chronic inflammation by modulating inflammatory gene expression and lipopolysaccharide levels. Lastly, dysbiosis can disrupt the circadian rhythm by affecting circadian transcription factors and epigenetic modifications, as well as bile and SCFA synthesis. These factors collectively increase the susceptibility to obesity.[49] Therefore, to explore the association between intestinal flora, short-chain fatty acids, and obesity, correlation analysis was performed.

The results of the correlation analysis indicated that the acetyl group was strongly positively correlated with viscosity, suggesting that the acetyl group in KGM may be a pivotal factor influencing its viscosity in the digestive tract. This

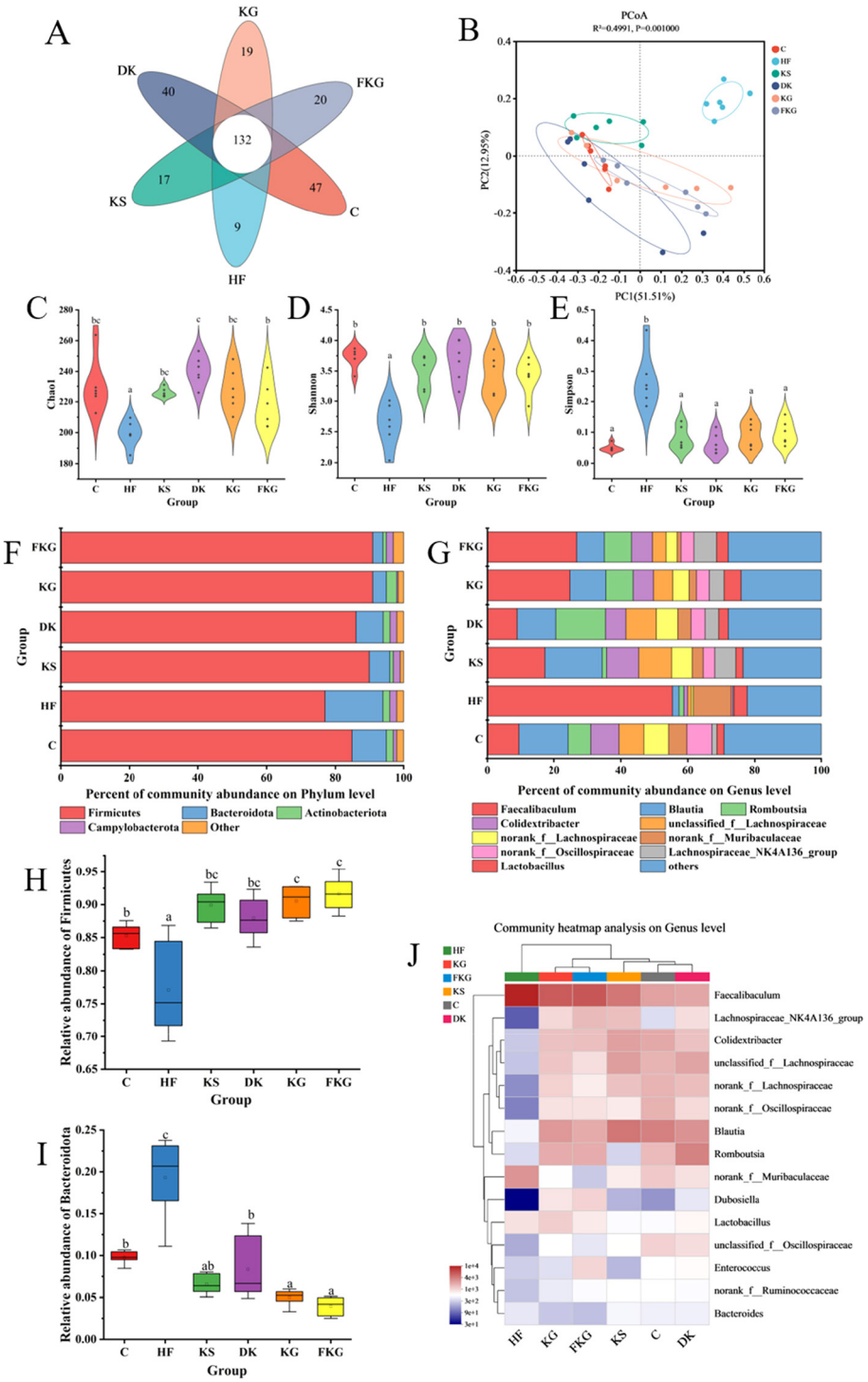

Fig. 14 Venn map (A), PCoA analysis of β diversity (B), α diversity analysis (C–E), phyla level species abundance (F), genus-level species abundance (G), Firmicutes relative abundance (H), Bacteroides relative abundance (I) and genus-level species composition heatmap (J) (n = 6).

finding aligns with previous studies and earlier sections of this research.[50] Furthermore, viscosity demonstrated a strong negative correlation with insulin resistance, TC, LDL-C, TNF-α, and the relative abundance of *Romboutsia* while showing a positive correlation with most SCFAs and the relative abundance of *Blautia* in feces.

SCFAs exhibited primarily positive correlations with HDL-C and GLP-1 and negative correlations with biochemical indicators including body weight, body fat, blood glucose, lipids, and inflammatory factors (Fig. 15). These findings suggest that SCFAs are beneficial for regulating glucose and lipid metabolism in obese mice.

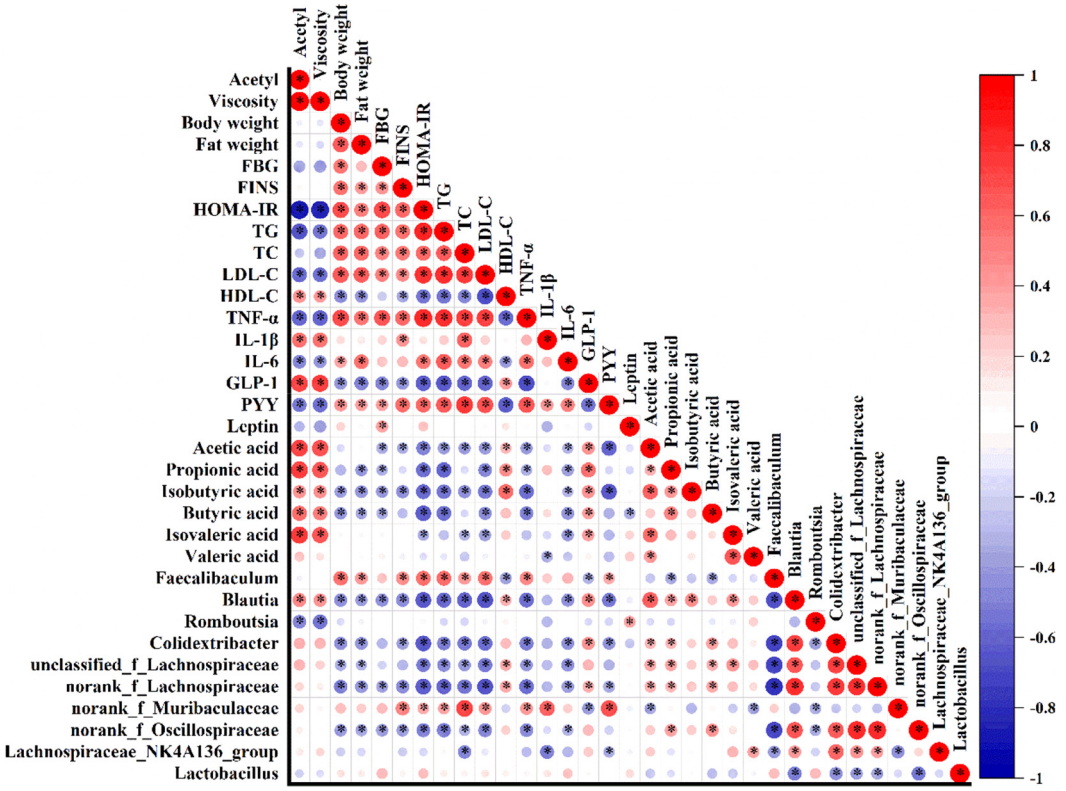

Fig. 15 Correlation analysis of basic biochemical indices, short-chain fatty acids and relative abundance of intestinal flora at the genus level; * indicates $p \leq 0.05$.

SCFAs were mainly associated with the relative abundance of *Faecalibaculum*, while *norank_f_Muribaculaceae* showed a negative correlation. However, there was a positive correlation between the relative abundances of *Lachnospiraceae_NK4A136_group*, *unclassified_f_Lachnospiraceae*, *Blautia*, *Colidextribacter*, *norank_f_Lachnospiraceae*, and *norank_f_Oscillospiraceae*.

The relative abundances of *norank_f_Muribaculaceae* and *Faecalibaculum* in the intestinal flora were significantly and positively correlated with body weight, body fat, blood glucose, and lipid levels. These findings suggest that the enrichment of *norank_f_Muribaculaceae* and *Faecalibaculum* in the intestinal microflora is detrimental to weight loss and the maintenance of glucose and lipid metabolism homeostasis. In contrast, the relative abundances of *norank_f_Oscillospiraceae*, *Blautia*, *Colidextribacter*, *unclassified_f_Lachnospiraceae*, and *norank_f_Lachnospiraceae* were significantly and negatively correlated with biochemical indices such as body weight, body fat, blood glucose, and lipids. These results indicate that the presence of these bacteria in the intestinal flora supports the maintenance of normal body weight, blood glucose, and lipid levels.

4. Conclusion

The intake pattern of konjac dietary fiber can influence the weight of obese mice to a certain extent, regulate the homeostasis of glucose and lipid metabolism, regulate the composition of intestinal flora, and improve intestinal flora disorders. Overall KS had the best effect on lowering blood glucose and fat. KS can increase the levels of fasting appetite hormones GLP-1 and PYY; up-regulate the mRNA expression of *LDLR*, *GCK* and *G-6-pase*; and increase the metabolic production of SCFAs by the intestinal flora in mice, thereby achieving better regulation of glucose and lipid metabolism. This study systematically explored the effects of different forms of KGM intake on body weight, body fat, glucose and lipid metabolism, and intestinal flora in high-fat obese mice, providing a theoretical basis for the development of KGM functional foods. However, the metabolic pathway of how KGM affects glucose and lipid metabolism through intestinal flora, appetite hormones, and inflammatory factors is still unclear.

Abbreviations

ALT	Alanine aminotransferase
AST	Aspartate transaminase
BW	Body weight
C	Control
CYP7A1	Cholesterol-7α-hydroxylase
DK	Deacetylated konjac glucomannan
FBG	Fasting blood-glucose
FINS	Fasting insulin
FKG	Frozen konjac glucomannan gel

FXR	Farnesol X receptor
G-6-pase	Glucose-6-phosphatase
GCK	Glucokinase
GLP-1	Glucagon like peptide-1
Glut4	Glucose transporter
GSK-3β	Glycogen synthase kinase 3β
HDL-C	High-density lipoprotein cholesterol
HF	High-fat diet
HOMA	Homeostatic model assessment
HOMA-IR	HOMA for insulin resistance
IL-1β	Interleukin-1β
IL-6	Interleukin 6
KG	Konjac glucomannan gel
KGM	Konjac glucomannan
KS	Konjac glucomannan sol
LDL-C	Low-density lipoprotein cholesterol
LDLR	Low density lipoprotein receptor
MDA	Malondialdehyde
OGTT	Oral glucose tolerance test
PEPCK	Phosphoenolpyruvate carboxykinase
PPARα	Peroxisome proliferators activate receptor alpha
PYY	Peptide tyrosine–tyrosine
SCFAs	Short chain fatty acids
SR-B1	Scavenger receptor B1
TC	Total cholesterol
TG	Triglycerides
TNF-α	Tumor necrosis factor-α

Author contributions

Sijia Zhu: conceptualization, formal analysis, data curation, writing – original draft, funding acquisition. Jiyu Yang: methodology, formal analysis, investigation, writing – original draft. Pengkui Xia: methodology, formal analysis, writing – review & editing. Sha Li: methodology, formal analysis. Qi Wang: methodology, formal analysis. Kaikai Li: conceptualization, methodology. Bin Li: conceptualization, methodology. Jing Li: conceptualization, methodology, writing – review & editing, supervision, funding acquisition.

Data availability

The data are available from the corresponding author on reasonable request.

Conflicts of interest

The authors declare no conflict of interest.

Acknowledgements

This work was financially supported by Hubei Provincial Natural Science Foundation for Distinguished Young Scholars (2022CFA085). We sincerely appreciate the help and support provided by the Experimental Animal Center of Huazhong Agricultural University.

References

1 Y. C. Chooi, C. Ding and F. Magkos, The epidemiology of obesity, *Metabolism*, 2019, **92**, 6–10.
2 A. Golden, Obesity's Impact, *Nurs. Clin. North Am.*, 2021, **56**, xiii–xiv.
3 The Writing Committee of the Report on Cardiovascular Health and Diseases in China and S. S. Hu, Report on cardiovascular health and diseases in China 2021: an updated summary, *J. Geriatr. Cardiol.*, 2023, **20**, 399–430.
4 B. Ahmed, R. Sultana and M. W. Greene, Adipose tissue and insulin resistance in obese, *Biomed. Pharmacother.*, 2021, **137**, 111315.
5 V. Ormazabal, S. Nair, O. Elfeky, C. Aguayo, C. Salomon and F. A. Zuñiga, Association between insulin resistance and the development of cardiovascular disease, *Cardiovasc. Diabetol.*, 2018, **17**, 122.
6 H. M. Roager and L. H. Christensen, Personal diet-microbiota interactions and weight loss, *Proc. Nutr. Soc.*, 2022, **81**, 243–254.
7 P. Portincasa, L. Bonfrate, M. Vacca, M. De Angelis, I. Farella, E. Lanza, M. Khalil, D. Q. Wang, M. Sperandio and A. Di Ciaula, Gut Microbiota and Short Chain Fatty Acids: Implications in Glucose Homeostasis, *Int. J. Mol. Sci.*, 2022, **23**, 1105.
8 H. D. Holscher, Dietary fiber and prebiotics and the gastrointestinal microbiota, *Gut Microbes*, 2017, **8**, 172–184.
9 B. Dalile, L. Van Oudenhove, B. Vervliet and K. Verbeke, The role of short-chain fatty acids in microbiota–gut–brain communication, *Nat. Rev. Gastroenterol. Hepatol.*, 2019, **16**, 461–478.
10 C. Zhang, J. D. Chen and F. Q. Yang, Konjac glucomannan, a promising polysaccharide for OCDDS, *Carbohydr. Polym.*, 2014, **104**, 175–181.
11 Y. Wang, K. Wu, M. Xiao, S. B. Riffat, Y. Su and F. Jiang, Thermal conductivity, structure and mechanical properties of konjac glucomannan/starch based aerogel strengthened by wheat straw, *Carbohydr. Polym.*, 2018, **197**, 284–291.
12 Y. Zhao, M. Jayachandran and B. Xu, In vivo antioxidant and anti-inflammatory effects of soluble dietary fiber Konjac glucomannan in type-2 diabetic rats, *Int. J. Biol. Macromol.*, 2020, **159**, 1186–1196.
13 S. Chearskul, S. Sangurai, W. Nitiyanant, W. Kriengsinyos, S. Kooptiwut and T. Harindhanavudhi, Glycemic and lipid responses to glucomannan in Thais with type 2 diabetes mellitus, *J. Med. Assoc. Thailand*, 2007, **90**, 2150–2157.
14 M. Yoshida, C. A. Vanstone, W. D. Parsons, J. Zawistowski and P. J. Jones, Effect of plant sterols and glucomannan on lipids in individuals with and without type II diabetes, *Eur. J. Clin. Nutr.*, 2006, **60**, 529–537.

15 G. S. Birketvedt, M. Shimshi, T. Erling and J. Florholmen, Experiences with three different fiber supplements in weight reduction, *Med. Sci. Monit.*, 2005, **11**, Pi5–Pi8.
16 T. Hozumi, M. Yoshida, Y. Ishida, H. Mimoto, J. Sawa, K. Doi and T. Kazumi, Long-term effects of dietary fiber supplementation on serum glucose and lipoprotein levels in diabetic rats fed a high cholesterol diet, *Endocr. J.*, 1995, **42**, 187–192.
17 R. F. Tester and F. H. Al-Ghazzewi, Beneficial health characteristics of native and hydrolysed konjac (Amorphophallus konjac) glucomannan, *J. Sci. Food Agric.*, 2016, **96**, 3283–3291.
18 X. Du, J. Li, J. Chen and B. Li, Effect of degree of deacetylation on physicochemical and gelation properties of konjac glucomannan, *Food Res. Int.*, 2012, **46**, 270–278.
19 J. A. Windeløv, J. Pedersen and J. J. Holst, Use of anesthesia dramatically alters the oral glucose tolerance and insulin secretion in C57Bl/6 mice, *Physiol. Rep.*, 2016, **4**, e12824.
20 X. Li, P. Chen, Y. Zhang, J. Zhang, S. Shen and K. Li, Intervention time modified the effect of inulin on high-fat diet-induced obesity and gut microbial disorders, *Food Front.*, 2023, 933–944.
21 M. Mathlouthi, Relationship between the structure and the properties of carbohydrates in aqueous solutions: solute-solvent interactions and the sweetness of D-fructose, D-glucose and sucrose in solution, *Food Chem.*, 1984, **13**, 1–16.
22 H. Zhang, M. Yoshimura, K. Nishinari, M. Williams, T. Foster and I. Norton, Gelation behaviour of konjac glucomannan with different molecular weights, *Biopolymers*, 2001, **59**, 38–50.
23 B. Li, J. Li, J. Xia, J. Kennedy, X. Yie and T. Liu, Effect of gamma irradiation on the condensed state structure and mechanical properties of konjac glucomannan/chitosan blend films, *Carbohydr. Polym.*, 2011, **83**, 44–51.
24 W. Lin, Y. Ni, L. Wang, D. Liu, C. Wu and J. Pang, Physicochemical properties of degraded konjac glucomannan prepared by laser assisted with hydrogen peroxide, *Int. J. Biol. Macromol.*, 2019, **129**, 78–83.
25 J. Chen, J. Li and B. Li, Identification of molecular driving forces involved in the gelation of konjac glucomannan: Effect of degree of deacetylation on hydrophobic association, *Carbohydr. Polym.*, 2011, **86**, 865–871.
26 C. L. Dikeman and G. C. Fahey, Viscosity as related to dietary fiber: a review, *Crit. Rev. Food Sci. Nutr.*, 2006, **46**, 649–663.
27 S. Ye, J. Zhu, B. R. Shah, Z. Abel Wend-Soo, J. Li, F. Zhan and B. Li, Preparation and characterization of konjac glucomannan (KGM) and deacetylated KGM (Da-KGM) obtained by sonication, *J. Sci. Food Agric.*, 2022, **102**, 4333–4344.
28 S. Wang, Y. Zhan, X. Wu, T. Ye, Y. Li, L. Wang, Y. Chen and B. Li, Dissolution and rheological behavior of deacetylated konjac glucomannan in urea aqueous solution, *Carbohydr. Polym.*, 2014, **101**, 499–504.
29 Y. Wu, R. Guo, N. Cao, X. Sun, Z. Sui and Q. Guo, A systematical rheological study of polysaccharide from Sophora alopecuroides L. seeds, *Carbohydr. Polym.*, 2018, **180**, 63–71.
30 C. Zhong and T. Langrish, A comparison of different physical stomach models and an analysis of shear stresses and strains in these system, *Food Res. Int.*, 2020, **135**, 109296.
31 L. Shang, Y. Wang, Y. Ren, T. Ai, P. Zhou, L. Hu, L. Wang, J. Li and B. Li, In vitro gastric emptying characteristics of konjac glucomannan with different viscosity and its effects on appetite regulation, *Food Funct.*, 2020, **11**, 7596–7610.
32 C. J. Rebello, C. E. O'Neil and F. L. Greenway, Dietary fiber and satiety: the effects of oats on satiety, *Nutr. Rev.*, 2016, **74**, 131–147.
33 M. Y. Li, G. P. Feng, H. Wang, R. L. Yang, Z. Xu and Y. M. Sun, Deacetylated Konjac Glucomannan Is Less Effective in Reducing Dietary-Induced Hyperlipidemia and Hepatic Steatosis in C57BL/6 Mice, *J. Agric. Food Chem.*, 2017, **65**, 1556–1565.
34 M. S. Wee, R. G. Lentle, K. K. Goh and L. Matia-Merino, The first of the viscoceuticals? A shear thickening gum induces gastric satiety in rats, *Food Funct.*, 2017, **8**, 96–102.
35 N. N. Wijayatunga and E. J. Dhurandhar, Normal weight obesity and unaddressed cardiometabolic health risk-a narrative review, *Int. J. Obes.*, 2021, **45**, 2141–2155.
36 J. X. Song, H. Ren, Y. F. Gao, C. Y. Lee, S. F. Li, F. Zhang, L. Li and H. Chen, Dietary Capsaicin Improves Glucose Homeostasis and Alters the Gut Microbiota in Obese Diabetic ob/ob Mice, *Front. Physiol.*, 2017, **8**, 602.
37 G. Marcelin, E. L. Gautier and K. Clément, Adipose Tissue Fibrosis in Obesity: Etiology and Challenges, *Annu. Rev. Physiol.*, 2022, **84**, 135–155.
38 H. Chen, Q. Nie, J. Hu, X. Huang, K. Zhang, S. Pan and S. Nie, Hypoglycemic and Hypolipidemic Effects of Glucomannan Extracted from Konjac on Type 2 Diabetic Rats, *J. Agric. Food Chem.*, 2019, **67**, 5278–5288.
39 A. Maia-Landim, J. M. Ramírez, C. Lancho, M. S. Poblador and J. L. Lancho, Long-term effects of Garcinia cambogia/Glucomannan on weight loss in people with obesity, PLIN4, FTO and Trp64Arg polymorphisms, *BMC Complementary Altern. Med.*, 2018, **18**, 26.
40 Y. Zheng, J. Li, X. Wang, M. Guo, C. Cheng and Y. Zhang, Effects of three biological combined with chemical methods on the microstructure, physicochemical properties and antioxidant activity of millet bran dietary fibre, *Food Chem.*, 2023, **411**, 135503.
41 F. Pietrocola and J. M. Bravo-San Pedro, Targeting Autophagy to Counteract Obesity-Associated Oxidative Stress, *Antioxidants*, 2021, **10**, 102.
42 H. P. Amin, C. Czank, S. Raheem, Q. Zhang, N. P. Botting, A. Cassidy and C. D. Kay, Anthocyanins and their physiologically relevant metabolites alter the expression of IL-6 and VCAM-1 in CD40L and oxidized LDL challenged vascular endothelial cells, *Mol. Nutr. Food Res.*, 2015, **59**, 1095–1106.
43 S. Chavarría-Arciniega, J. C. López-Alvarenga, N. O. Uribe-Uribe, M. Herrera-Hernández and J. González-Barranco, [Relationship between morphological diagnosis of NASH

(non-alcoholic steatohepatitis) and liver function tests in a group of patients with morbid obesity], *Rev. Invest. Clin.*, 2005, **57**, 505–512.

44 C. Liu, M. Shao, L. Lu, C. Zhao, L. Qiu and Z. Liu, Obesity, insulin resistance and their interaction on liver enzymes, *PLoS One*, 2021, **16**, e0249299.

45 I. N. Grigor'eva, Gallstone Disease, Obesity and the Firmicutes/Bacteroidetes Ratio as a Possible Biomarker of Gut Dysbiosis, *J. Pers. Med.*, 2020, **11**, 13.

46 M. Duan, Y. Wang, Q. Zhang, R. Zou, M. Guo and H. Zheng, Characteristics of gut microbiota in people with obesity, *PLoS One*, 2021, **16**, e0255446.

47 W. Cai, J. Xu, G. Li, T. Liu, X. Guo, H. Wang and L. Luo, Ethanol extract of propolis prevents high-fat diet-induced insulin resistance and obesity in association with modulation of gut microbiota in mice, *Food Res. Int.*, 2020, **130**, 108939.

48 K. Hosomi, M. Saito, J. Park, H. Murakami, N. Shibata, M. Ando, T. Nagatake, K. Konishi, H. Ohno, K. Tanisawa, A. Mohsen, Y. A. Chen, H. Kawashima, Y. Natsume-Kitatani, Y. Oka, H. Shimizu, M. Furuta, Y. Tojima, K. Sawane, A. Saika, S. Kondo, Y. Yonejima, H. Takeyama, A. Matsutani, K. Mizuguchi, M. Miyachi and J. Kunisawa, Oral administration of Blautia wexlerae ameliorates obesity and type 2 diabetes via metabolic remodeling of the gut microbiota, *Nat. Commun.*, 2022, **13**, 4477.

49 B. N. Liu, X. T. Liu, Z. H. Liang and J. H. Wang, Gut microbiota in obesity, *World J. Gastroenterol.*, 2021, **27**, 3837–3850.

50 X. D. Shi, J. Y. Yin, S. W. Cui, Q. Wang, S. Y. Wang and S. P. Nie, Comparative study on glucomannans with different structural characteristics: Functional properties and intestinal production of short chain fatty acids, *Int. J. Biol. Macromol.*, 2020, **164**, 826–835.